EDGE ARTICLE

Check for updates

Picking the tyrosine-lock: chemical synthesis of the tyrosyl-DNA phosphodiesterase I inhibitor recifin A and analogues†

Taylor B. Smallwood, [a] Lauren R. H. Krumpe, [b] Colton D. Payne, [a] Victoria G. Klein, ‡[c] Barry R. O'Keefe, [bd] Richard J. Clark, *[a] Christina I. Schroeder *[ce] and K. Johan Rosengren *[a]

The peptide recifin A is the inaugural member of the structurally intriguing new fold referred to as a tyrosine-lock. Its central four stranded β-sheet is stabilized by a unique arrangement in which three disulfide bonds and their interconnecting backbone form a ring that wraps around one of the strands, resulting in a Tyr side chain being buried in the molecular core. Here we aimed to establish a synthetic route to this complex class of natural products. Full length recifin A was successfully generated through native chemical ligation chemistry joining two 21 amino acid residue fragments. Surprisingly, reduced linear recifin A readily adopts the correct, topologically-complex fold via random oxidation of the cysteines, suggesting it is highly energetically favored. Utilizing our synthetic strategy, we generated five recifin A analogues to investigate the structural role of the central Tyr residue and provide the first insights into the structure activity relationship of recifin A towards its cancer target tyrosyl-DNA phosphodiesterase I.

Introduction

Marine sponges are a diverse source of unique natural products, with many containing bioactive peptides and proteins. These molecules possess a wide range of pharmacological effects including cytotoxic and anticancer activities.[1,2] Recently a novel peptide, recifin A, was isolated from the marine sponge *Axinella* sp. during a screening campaign to identify inhibitors of the enzyme tyrosyl-DNA phosphodiesterase 1 (TDP1).[3] TDP1 is a DNA repair enzyme that recognizes stalled DNA-topoisomerase 1 (TOP1)/DNA covalent complexes and catalyzes the hydrolysis of the 3′-phosphodiester bond.[4] Clinically, TDP1 can reduce the impact of chemotherapeutic TOP1 inhibiting drugs, such as the camptothecin derivates topotecan and

irinotecan, resulting in diminished DNA damage and reduced efficacy of this class of anti-tumor agents.[5] Therefore, chemotherapy using TOP1 inhibitors in combination with TDP1 inhibitors could be a promising new avenue for clinical cancer treatment.

Recifin A is the first described peptidic and allosteric inhibitor of TDP1.[3] Unlike previous small molecule TDP1 inhibitors that target the active site located in the C-terminal catalytic domain of TDP1, recifin A requires the presence of the unstructured N-terminal regulatory domain of TDP1 for its inhibitory activity. Recifin A comprises 42 amino acid residues, and solution Nuclear Magnetic Resonance (NMR) spectroscopy studies revealed that it is the first member of a new structural family of cysteine-rich peptides, named the Tyr-lock family of peptides.[3] The recifin A secondary and tertiary structure is stabilized by three disulfide bonds, Cys⁵–Cys²¹, Cys¹¹–Cys³⁹ and Cys²²–Cys⁴², a I–III, II–V, IV–VI arrangement (Fig. 1). Peptides with three disulfide bonds often form topologically complex arrangements referred to as inhibitory cystine knots, with a I–IV, II–V, III–VI disulfide bond arrangement, in which two disulfide bonds and their interconnecting backbone form a ring through which the third disulfide bond is threaded.[6,7] However, what is unique about the recifin A structure is that all three disulfide bonds together with backbone segments form a ring that wraps around the third β-strand (residues 27–29). The fold of the peptide is further stabilized by Tyr⁶, which is deeply buried in the peptide core and locked in place by interactions with surrounding residues (Fig. 1).

[a]*The University of Queensland, School of Biomedical Sciences, Brisbane, QLD, 4072, Australia. E-mail: richard.clark@uq.edu.au; j.rosengren@uq.edu.au*

[b]*Molecular Targets Program, Centre for Cancer Research, National Cancer Institute, National Institute of Health, Frederick, MD, 21702, USA*

[c]*Chemical Biology Laboratory, Centre for Cancer Research, National Cancer Institute, National Institute of Health, Frederick, MD, 21702, USA*

[d]*Natural Products Branch, Centre for Cancer Research, National Cancer Institute, National Institute of Health, Frederick, MD, 21702, USA*

[e]*Peptide Therapeutics, Genentech Inc, 1 DNA Way, South San Francisco, CA, 94080, USA. E-mail: Schroeder.christina@gene.com*

† Electronic supplementary information (ESI) available: HPLC traces, MS data, NMR data. See DOI: https://doi.org/10.1039/d4sc01976h

‡ Current address: Laboratory of Bioorganic Chemistry, National Institute for Diabetes and Digestive Kidney Diseases, National Institute of Health, Bethesda, MD, 20892, United States.
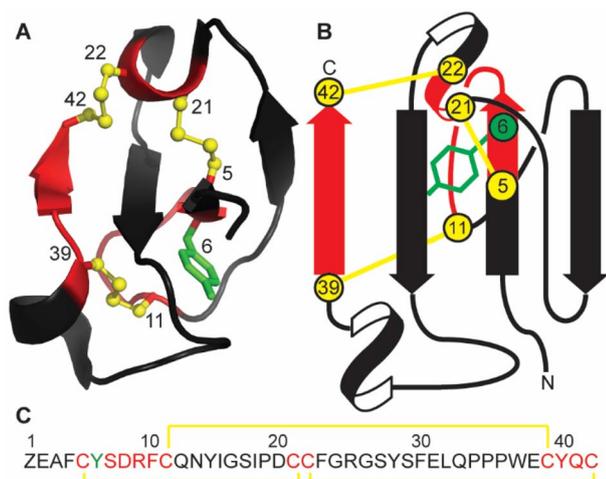
Fig. 1 (A) Ribbon structure of recifin A showing the position of the buried Tyr[6]. (B) Schematic illustration showing threading of the third β-strand through the embedded ring formed by the three disulfide bonds. (C) The recifin A amino acid sequence. In all panels the disulfide bonds are highlighted in yellow, residues that form the ring in red, Tyr[6] in green, and remaining residues in black. Z in the sequence represents pyroglutamate.

Scheme 1 Synthetic strategy for recifin A using native chemical ligation of a C-terminal thioester produced by hydrazide chemistry and an N-terminal cysteine. Z – pyroglutamate.

For natural products, accessing sufficient native material for detailed activity and structural studies is often challenging. In the case of recifin A, to be able to further investigate the interaction between this peptide and TDP1, synthetic material is required. In this work we therefore focused on establishing a synthetic route for the production of recifin A, to allow for the generation of analogues, and to expand our knowledge of the key structural requirements of the Tyr-lock fold. We show that the linear recifin A can be assembled through ligation chemistry and efficiently oxidized to the correct disulfide isomer despite the complex fold. Functional data from analogues suggest that the TDP1 binding surface is extensive and that the buried tyrosine residue is critical for structural stability and consequently activity.

Results and discussion

Initial attempts at assembling the full-length recifin A *via* Fmoc-chemistry on 2-chlorotrityl resin were unsuccessful. Instead, it was necessary to employ a chemical ligation strategy. We chose to split the sequence between the central consecutive cysteines into two 21 amino acid fragments, and employ a native chemical ligation (NCL)[8] strategy in which the C-terminal thioester was produced through hydrazide chemistry (Scheme 1).[9,10] Individual N- and C-terminal recifin A fragments were successfully synthesized (Fig. S1 and Table S1†), and could be efficiently ligated into the full length peptide (Fig. S2†). The linear reduced peptide was subjected to thermodynamic oxidative folding using ammonium bicarbonate buffer in the presence of reduced and oxidized glutathione. Surprisingly, despite the expected complexity required for correct folding, a single dominant product appeared almost immediately under
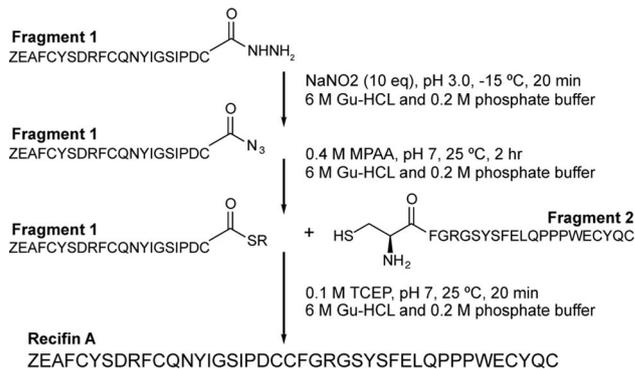
these conditions. This product was obtained in high purity after HPLC purification (Fig. S3†) and solution NMR spectroscopy revealed a well dispersed ^{1}H NMR spectrum, implying that the peptide adopted an ordered structure in solution (Fig. S4†).

The native isolated recifin A and the synthetic version were compared using LC/MS analysis. Individual RP-HPLC analysis of the two peptides found they possessed the same retention time, and a co-elution experiment of the native and the synthetic recifin A showed no difference in retention time or peak shape (Fig. 2A). Comparing the two recifin A peptide's molecular charge envelope, identical ionization patterns and distribution of charge states were observed, with essentially identical isotopic distribution of $[M + 3H]^{3+}$ (Fig. S5†). Furthermore, 2D NMR spectra including TOCSY and NOESY were recorded for synthetic recifin A and compared to the data used for structure determination of the native peptide, showing conserved peak patterns and positions (Fig. 2B). It should be noted that the NMR data of recifin A is highly sensitive to minute changes in pH conditions and concentration, making it difficult to replicate conditions perfectly. Consequently, some minor differences in chemical shifts are observed. A closer analysis of the chemical shifts and the recifin A structure
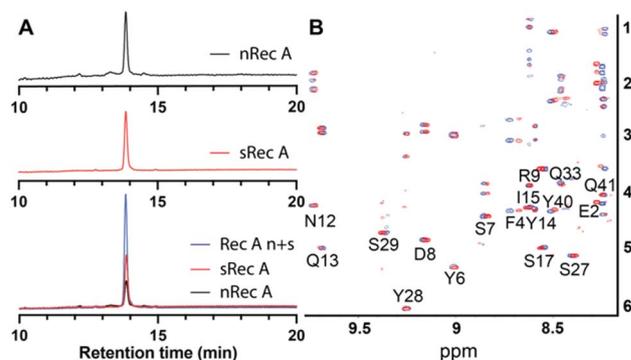

Fig. 2 (A) Comparison of elution times of native (nRec A, red) and synthetic (sRec A, blue) recifin A and co-elution of native and synthetic recifin A (Rec A n + s, black). (B) Superposition of TOCSY spectra of native (red) and synthetic (blue) recifin A at 298 K.

revealed that any resonance with a notable perturbation is in close proximity to a titratable group, most prominently Glu[31] and Glu[38], thus sensing their respective protonation state. Altogether, these data verify that the synthetic recifin A possesses the same chemical properties as the isolated peptide.

Based on the structure of the native recifin A peptide, we designed and synthesized five analogues (Fig. 3) to investigate the effects of the mutations on the peptide structure and activity. We first designed two peptides with mutations at the N-terminus. Recifin (3–42) is a truncated version of the native peptide, removing the first two N-terminal residues, pyroglutamic acid and glutamic acid. The [Pro[1]] recifin analogue replaces the N-terminal pyroglutamic acid residue with another five membered ring residue, proline. Next, we designed two analogues with modifications at Tyr[6], the structurally important residue responsible for sterically stabilizing the native recifin A peptide core. This was conservatively replaced with another aromatic residue, phenylalanine ([Phe[6]] recifin), and with the smaller aliphatic residue alanine ([Ala[6]] recifin). The final recifin A analogue that was designed was [Ala[10]] recifin, where the surface-exposed Phe[10] was replaced with Ala. Phenylalanine residues are rarely found on the surface of proteins, unless they are involved in intermolecular interactions.[11,12] Therefore, it was hypothesized that Phe[10] may be a key binding residue and involved in protein–protein interactions between recifin A and the regulatory domain of TDP1.

Each recifin analogue was synthesized using the established hydrazide NCL methodology and folded under the same conditions as the synthetic recifin A (Fig. S1–S3 and Table S1†). All peptide analogues, apart from [Ala[6]] recifin, were found to oxidise into one isomer, which was confirmed by NMR spectroscopy to be correctly folded (Fig. S4†). Fig. 4 shows the comparison of the oxidative folding of native recifin A and [Phe[6]], highlighting that even with a change at this key position the correct fold is remarkably favoured. In contrast, folding of [Ala[6]] recifin resulted in multiple isomers and this analogue could not be purified to homogeneity (Fig. S3†). The 1D ^{1}H NMR spectrum of partially purified peptide showed broad peaks lacking the wide dispersion characteristic of the recifin A fold, indicating that this variant was misfolded (Fig. S4†). The structures of all analogues, except for [Ala[6]] recifin, were further analyzed by 2D NMR spectroscopy. Secondary H_α chemical shifts revealed that the secondary structural features follow the same trend to that of the native recifin A peptide (Fig. S6†). All peptides were shown to possess a series of short β-strands and
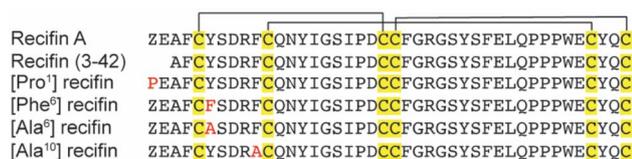

Fig. 4 Oxidative folding of (A) recifin A and (B) [Phe[6]] recifin. HPLC traces of each time point taken for the oxidation of synthetic peptides. Oxidation was performed in 0.1 M ammonium bicarbonate (pH 8.0) with oxidized (0.5 mM) and reduced (2 mM) glutathione at a concentration of 0.125 mg mL^{-1} at room temperature. Aliquots were removed at time points 0, 8, and 48 h, quenched with 6 M Gu-HCl (pH 3.7). Samples were analyzed by analytical RP-HPLC on a C18 column using a gradient of 5% buffer B for the first 10 min followed by 5–65% B (buffer A: H$_2$O/0.05% TFA; buffer B: 90% ACN/10% H$_2$O/0.045% TFA) in 65 min.

α-helices/turns, as indicated by significant stretches of positive and negative secondary chemical shifts, respectively.

[Phe[6]] recifin was structurally investigated in more detail, given the peptide was able to fold despite a change to the class-defining Tyr[6]. Calculating a three-dimensional structure of [Phe[6]] recifin revealed a structure with essentially identical backbone conformation to native recifin A (Fig. 5). The key features in the Tyr-lock region observed in the native recifin A structure is maintained in the [Phe[6]] recifin analogue. Like in the native recifin A individual resonance signals are observed for the aromatic protons, resulting from the ring-flips being slowed down by the same steric packing. The removal of the Tyr[6] hydroxyl group does however result in the loss of two hydrogen bonds. In recifin A it both donates a hydrogen bond to the backbone carbonyl of Glu[31] and accepts a hydrogen bond from the backbone amide of Gln[33]. The lack of these interactions stabilizing this region results in increased dynamics, evident from significant line broadening of the backbone

Fig. 3 Aligned sequences of recifin A and analogues. Conserved cysteine residues are shown in yellow, with the black line highlighting the disulfide bond connection: Cys I–III, Cys II–V, and Cys IV–VI. Point mutations are shown in red. Z = pyroglutamic acid.
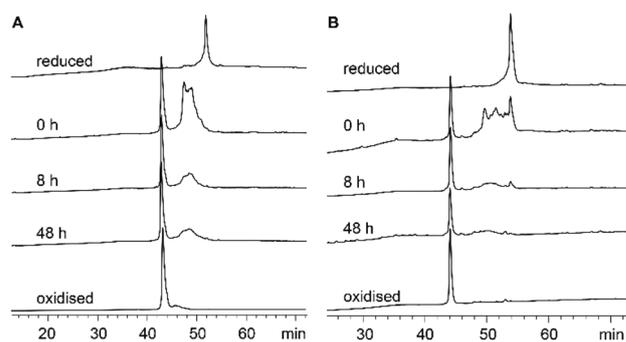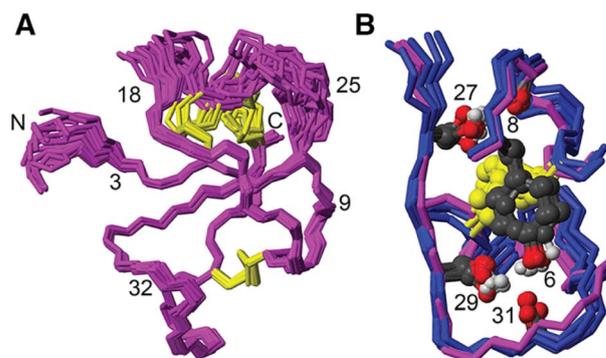

Fig. 5 (A) Solution NMR structure of [Phe[6]] recifin showing disulfides in yellow. (B) Superposition of [Phe[6]] recifin (pink) and native recifin A (blue) (PDB ID: 6XN9), highlighting the similarities in the Tyr-lock region and hydrogen bonds.

amides of residues 30–33. Interestingly two other side chain hydrogen bonds in the region, from Ser[27] to Glu[8] carbonyl and from Ser[29] to Glu[31] carbonyl are maintained, as these hydroxyl protons remain visible in the spectra, like in native recifin A. Thus, while the aromatic ring of the Phe residue is sufficient to maintain the so-called Tyr-lock, increased dynamics surrounding this region and minor differences in the backbone conformation of residues 31–33 are evident.

To evaluate the thermal stability for native and synthetic recifin A and analogues, we collected 1D ^{1}H NMR spectra at increasing temperatures in 10 °C increments (20–60 °C) at 15 min intervals. Following collection of the final spectra at 60 °C, we allowed the sample to cool and collected an additional spectrum at 20 °C (Fig. S7†). Whilst we observed some expected chemical shift changes in the amide region with increased temperature, we did not observe any noticeable temperature dependent line broadening for any of the peptides, and the final spectra collected at 20 °C were identical to the initial spectra. This suggests that the β-sheets in combination with the complex disulfide bond framework renders these peptides highly stable towards thermal assault.

To investigate if our designed modifications had functional effects in terms of ability to inhibit TDP1, native recifin A and all synthetic analogs were tested side-by-side in a fluorescence resonance energy transfer (FRET) assay system. Native isolated recifin A was found to inhibit full-length TDP1 enzymatic activity in a concentration dependent manner with an IC$_{50}$ of 0.80 μM, moderately higher than initially reported.[2] The synthetic recifin A peptide and [Pro[1]] recifin were also found to inhibit TDP1 with equivalent potency (0.58 and 0.69 μM, respectively) in our assay, as shown in Table 1 and Fig. S8.† Surprisingly, neither [Phe[6]] recifin nor [Ala[10]] recifin showed any inhibition of TDP1 at the highest test dose of 10 μM, and the truncated analogue recifin 3–42, was also found to have no measurable TDP1 inhibitory activity. This suggests that recifin A engages TDP1 using an extended binding surface given that the N-terminal part of recifin A and Phe[10] are spatially separated, yet both are important for TDP1 inhibitory activity. Since the replacement of the N-terminal pyroglutamic acid with Pro was tolerated the reduced binding of the truncated analogue is likely a result of the removal of the Glu[2] negatively charged side chain. Thus, the interaction likely involves both charge attraction and hydrophobic packing. Importantly, recifin A requires the disordered N-terminal regulatory domain of TDP1 for activity,[2] and these findings are consistent with an interaction in which this disordered region 'wrap around' recifin A, creating the extended binding surface. Alternatively, recifin A might be

'sandwiched' between the regulatory and catalytic domains, thus being involved in multiple interactions. Either arrangement could explain why reducing the rigidity and increasing structural dynamics by replacing the buried Tyr[6] with a Phe is sufficient to reduce activity, despite this modification not directly affecting the peptide surface, as evident from our NMR structure. Further variants are required to be produced to explore the structure–activity relationship between recifin A and TDP1. Notable putative interaction surfaces include Arg[9] and Arg[25], which are adjacent to Phe[10], and the aromatic cluster involving Tyr[28], Phe[30] and Tyr[40] located proximal to the N-terminus.

Experimental

Materials

Peptide synthesis

Native recifin A and analogues thereof could not successfully be assembled in one fragment using Fmoc solid phase peptide synthesis (SPPS) despite modifications to resin loading, coupling times and reagent equivalents used. Therefore, a native chemical ligation (NCL) approach using peptide hydrazides was applied to ligate the N- and C-terminal fragments between the 3rd and the 4th cysteine residues. This site was chosen as it is located at the center of the sequence, whereas all other cysteines are concentrated towards the N-terminus or C-terminus. An NCL could not be performed between Asp[20] and Cys[21] due to potential cyclisation between the sidechain carboxylic of Asp[20] and the C-terminal hydrazide.[9]

N-terminal fragment 1 hydrazide synthesis. The peptide hydrazide fragment was synthesized following the protocol established by Liu et al.[10] Briefly, 2-Cl-(Trt)-Cl (0.5 mmol scale) was washed with DMF three times, DCM three times and DMF three times. The resin was swelled in 50% (v/v) DMF/DCM for 30 min. After, the solution was drained and 5% (v/v) freshly made NH$_2$NH$_2$ in DMF was added to the resin for hydrazination. The mixture was gently agitated for 30 min at room temperature. The resin was then washed with DMF and DCM three times before repeating incubation with 5% (v/v) freshly made NH$_2$NH$_2$ in DMF for 30 min. After 30 min the resin was washed with DMF and DCM three times before 5% (v/v) MeOH/DMF was added to the resin which was agitated for 10 min to cap unreacted sites. Finally, the resin was washed with DMF

Table 1 Inhibition of TDP1 by recifin A and analogues

Peptide	IC$_{50}$ μM	95% CI	R^2
Native recifin A	0.80	0.08–7.93	0.90
Synthetic recifin A	0.58	0.20–1.77	0.96
Recifin A (3–42)	>10	ND	ND
[Pro[1]] recifin A	0.69	0.26–1.88	0.97
[Ala[10]] recifin A	>10	ND	ND
[Phe[6]] recifin A	>10	ND	ND

three times, DCM three times and DMF three times before manual coupling of the first amino acid. Cys(Trt) (4 eq.) was coupled to the hydrazine resin with HBTU (4 eq.) and DIPEA (8 eq.) for 2 × 1 h. The remainder of fragment 1 for native recifin A and analogues were synthesized using Fmoc chemistry on a CS136X synthesizer (CSBio), with a coupling time of 30 min at 40 °C using HBTU (0.4 M) and DIPEA (0.8 M) as coupling reagents.

C-terminal fragment 2 synthesis. 2-Cl-(Trt)-Cl (0.25 mmol scale) was swelled in DCM for 30 min before manual addition of Cys(Trt) (4 eq.) in DCM and DIPEA (8 eq.). A few drops of DMF were added to dissolve the amino acid completely. The amino acid was coupled for 2 × 1 h. The remainder of fragment 2 was synthesized using Fmoc chemistry on a CS136X synthesizer (CSBio), with a coupling time of 30 min at 40 °C using HBTU (0.4 M) and DIPEA (0.8 M) as coupling reagents.

Peptide cleavage. N-terminal hydrazide peptide fragment 1 and C-terminal peptide fragment 2, were cleaved from the resin using TFA with DODT, TIPS, and H_2O as scavengers (90 : 5 : 2.5 : 2.5) at room temperature for 2 h. TFA was removed under vacuum and peptide precipitated with ice-cold diethyl ether. The precipitate was filtered and dissolved in 50% ACN containing 0.05% TFA. The remaining diethyl ether was removed under vacuum and the peptide solution lyophilized. Crude peptides were purified by reverse phase-HPLC (RP-HPLC) on a C18 column (Phenomenex Jupiter 300 Å, 10 μm, 250 × 21.2 mm) using a gradient of 0–90% B (buffer A: 0.05% TFA; buffer B: 90% ACN/0.045% TFA) in 90 min at a flow rate of 8 mL min^{-1}. Electrospray ionization-mass spectroscopy (ESI-MS) with declustering potential set to 40 was used to confirm the molecular mass of the synthesized peptide fragments using an ABSciex API2000 before lyophilization (Fig. S1†).

Native chemical ligation. N-terminal hydrazide peptide fragments 1-NHNH$_2$ (1 mM) were dissolved in 1 mL of ligation buffer (6 M Gu-HCl, 0.2 M phosphate buffer) and pH was adjusted to ~3 with 1 M HCl. The peptide solution was cooled in a −15 °C ice/salt bath (12 g NaCl to 50 g of ice) before the addition of NaNO$_2$ (10 eq.). The peptide solution was gently agitated for 20 min while cooled in the ice bath to convert the peptide hydrazide to the corresponding azide (N-terminal fragment 1-N$_3$). 0.4 M MPAA was dissolved in 1 mL of ligation buffer and pH was adjusted to 6.8 with 10 M NaOH. C-terminal peptide fragment 2-COOH (1 mM) was dissolved in the 0.4 M MPAA solution and added to the N-terminal fragment 1-N$_3$ solution. The ligation mixture was brought to room temperature and pH was slowly adjusted to 7 using 1 M NaOH. The ligation reaction was left at room temperature for 2 h and monitored using liquid chromatography-mass spectrometry (LC-MS). Upon completion of the reaction, the ligation solution was reduced in 10 mL of 6 M Gu-HCL and 0.1 M TCEP and incubated for 20 min. After, the ligation solution was diluted tenfold with deionized H_2O before being filtered and purified by RP-HPLC on a C18 column using a gradient of 0–90% B in 90 min. ESI-MS with declustering potential set to 40 was used to confirm the molecular mass of the ligated peptides before lyophilization (Fig. S2†).

Table 2 Experimental yields for recifin A peptides

Peptide	% Yield[a]
Recifin A N-terminal fragment	27
Recifin A C-terminal fragment	21
Ligated reduced recifin A	30
Folded recifin A	56

[a] Isolated yield after HPLC purification.

Disulfide bond formation. Pure reduced ligated peptides were dissolved in 0.1 M NH$_4$HCO$_3$ buffer (pH 8) with oxidized (0.5 mM) and reduced (2 mM) glutathione at a concentration of 0.125 mg mL^{-1} for 48 h at room temperature. Aliquots of 10 μL were taken at timepoint intervals (0 h, 30 min, 1 h, 2 h, 4 h, 6 h, 8 h, 24 h and 48 h) and quenched in 10 μL 6 M Gu-HCl (pH 3.7). Samples were analyzed by analytical RP-HPLC on a C18 column using a gradient of 5% buffer B for the first 10 min followed by 5–65% B in 65 min. Oxidized peptides were purified by RP-HPLC on a C18 column using a gradient of 0–90% B in 90 min. ESI-MS with declustering potential set to 40 was used to confirm the molecular mass of the oxidized peptides before lyophilization. Analytical RP-HPLC was used to confirm peptide purity (Fig. S3†). Typical yields for the different synthesis steps are given in Table 2.

LC-MS analysis of native and synthetic recifin A

Peptides were analyzed on an Agilent Q-TOF LC-MS system as previously described.[3] Briefly, approximately 250 ng of peptide was injected onto an Poroshell 300SB-C18, 5 μm, 2.5 × 75 mm analytical HPLC column, heated to 40 °C and equilibrated in H_2O/0.1% formic acid (A). A linear gradient from 100% A to 60% ACN + 0.1% formic was executed at a flow rate of 1 mL min^{-1} over 5 min to elute the peptides, followed by a 1 min gradient to 100% ACN + 0.1% formic acid. Spectra were collected within 100–3200 *m/z* range at 1 spectra per s, with internal reference mass correction at 121.05 and 1221.99 *m/z*. Peptide mass spectra were deconvoluted for mass determination using Agilent BioConfirm data analysis software (Fig. S5†).

RP-HPLC co-elution of native and synthetic recifin A

Native, synthetic recifin A and a mixture of both peptides were analyzed for retention time using a Shimadzu Nexera RP-HPLC equipped with a LC-20AD pump and a SPD-M30A diod array detector on a Phenomenex Gemini column NX-C18 (5 μm, 110 Å) using a 0–60% B gradient over 20 min (buffer A: 0.05% TFA, buffer B: 90% ACN/0.045% TFA).

NMR spectroscopy

Recifin analogues were dissolved in 90% H_2O/10% D_2O at a concentration of 1 mM, pH ~4.9. Standard one- and two-dimensional data sets were recorded at 298 K on a Bruker Avance III 900 MHz spectrometer equipped with a cryoprobe and processed with Topspin 4.0.3 (Bruker Biospin), with data referenced to the residual water signal at 4.77 ppm. ^1H–^1H TOCSY[13] (Total Correlation Spectroscopy) and NOESY[14] (Nuclear Overhauser Spectroscopy) experiments were recorded with

a sweep width of 12 ppm, 512 increments, and mixing times of 80 and 150 ms, respectively. TOCSY experiments were recorded with four scans and NOESY experiments with 32 scans. Additional ^{1}H–^{13}C and ^{1}H–^{15}N HSQC (Heteronuclear Single Quantum Coherence spectroscopy) spectra were recorded at natural abundance for [Phe[6]] recifin. ^{1}H–^{13}C HSQC data was recorded with 96 scans and 200 increments for and ^{15}N data was recorded with 128 scans and 128 increments. The program CARA[15] (Computer Aided Resonance Assignment) was used to assign the data using sequential assignment strategies[16] and derive structural information.[17] Analysis of the secondary structural features of the recifin analogues was achieved by direct comparison of each analogues secondary H_{α} shifts to that of native recifin. Secondary H_{α} shifts were determined by comparison of the observed chemical shift of each H_{α} proton to that of the equivalent random coil value.[18] Additional TOCSY data were recorded at varying temperatures (288, 293, 298, 303 and 308 K) for [Phe[6]] recifin to monitor the temperature dependence of the backbone amide protons.

Structure calculations. The [Phe[6]] recifin analogue was chosen for structure calculation. The structure of this analogue was calculated using both inter-proton distance restraints generated from NOESY cross peak volumes and dihedral Φ (C_{-1}–N–C_{α}–C) and ψ (N–C_{α}–C–N_{+1}) backbone angles generated using chemical shifts by TALOS-N[19] (torsion angle likelihood obtained from shift and sequence similarity). Hydrogen bond restraints were identified through the combination of amide temperature coefficients,[20] to determine donors, and preliminary structure calculations, to determine acceptors. Initial structures (50) were generated using CYANA 3.98.5 [21] and final structures were subjected to simulated annealing and refined in explicit water using CNS 1.21.[22] Stereochemical analysis was conducted by MolProbity[23] by comparing the generated [Phe[6]] recifin structures to that of structures published in the Protein Data Bank (PDB ID: 6XN9). The 20 best structures which contained no violations of distances or dihedral angles above 0.2 Å or 2°, and had low energy were chosen to represent the structure of [Phe[6]] recifin (Table S2†). MOLMOL[24] was used to generate images of the secondary and tertiary structure of [Phe[6]] recifin. The structures, restraints, and chemical shifts have been submitted to the PDB and BRMB (Biological Magnetic Resonance Bank), the accessions codes are (8V2V) and (31130), respectively.

Thermal stability analysis. Thermal stability of native recifin A, synthetic recifin A and synthetic recifin A analogues was carried out using nuclear magnetic resonance on a 500 or 700 MHz Bruker Avance III equipped with a cryoprobe. Sample concentrations were 0.2–1 mg mL^{-1}, pH ranged from 5.8–7.59 and the number of scans were 256–1024. 1D ^{1}H NMR were run at 293 K and at increasing temperatures at 10 K intervals (293–333 K) followed by a final spectrum acquired at 293 K to ensure that any structural changes brought about by elevated temperatures were temporary and reversible (Fig. S7†).

FRET-based TDP1 enzymatic activity inhibition assay

The FRET-based TDP1 enzymatic activity assay is based on the removal of an eosin-linked phospho-tryosyl fluorophore from the 3′ end of the DNA substrate (TAMRA-5′-GATCTAAAAGACTT-pY-3′-eosin) by TDP1 which results in an increase in fluorescence from the 5′-linked TAMRA substrate. The assay has been described in detail previously but was slightly modified for this study.[3] Briefly, 3-fold concentrated dilution series of peptides, TDP1 enzyme, and FRET substrate were prepared in FRET buffer (1X PBS pH 7.4, 80 mM KCl, 1 mM TCEP). TDP1, peptides, and substrate were then added sequentially to wells of a black, 384-well plate (Greiner 784900), mixed to combine, and analysed for one hour (520 nm$_{ex}$/550 nm$_{em}$). Assay concentrations of TDP1 and FRET substrate were 1 nM and 0.25 μM, respectively. Results were normalized to assay controls (no TDP1 and un-inhibited TDP1), and dose–response curves and IC$_{50}$ estimates were generated using Graph-Pad Prism software non-linear regression tools based on the 15 min timepoint (least squares fit with three parameters).

Conclusions

We have here described the first chemical synthesis of the novel allosteric TDP1 inhibitor, recifin A, the inaugural member of the new Tyr-lock fold. We have shown that recifin A and analogues can readily be synthesized using hydrazide native chemical ligation methodology and that recifin A folds into primarily one species probably driven by the complex disulfide bond network folding around a buried aromatic residue. Evaluation of an initial series of recifin A analogues revealed that the central Tyr[6] residue, giving the family its name, can be replaced with a Phe without significant changes in folding or 3D structure, but that it does increase structural dynamics and results in reduction of TDP1 inhibition potency. In contrast, replacing Tyr[6] with an Ala is detrimental for folding. We also showed that replacing the N-terminal pyroglutamic acid with a Pro, [Pro[1]] recifin, did not alter activity, but that truncating the first two residues recifin (3–42), resulted in drastic reduction in inhibition of TDP1. Having established a synthetic route for recifin A opens the door for synthesis of further analogues enabling detailed studies of the allosteric mechanism by which recifin A inhibits TDP1. Understanding allosteric inhibition of TDP1 could lead to design of novel and selective TDP1 inhibitors sensitizing cells to TOP1 inhibitors for the treatment of cancer.

Author contributions

TBS, LRHK, CDP, VGK – investigation, formal analysis, writing original draft. BRO, RJC, CIS, KJR – conceptualization, formal analysis, project administration, resources, writing original draft, writing – review and editing.

Conflicts of interest

LRHK, BRO, CIS and KJR are co-inventors on a patent relating to tyrosyl-lock peptides. CIS is a Genentech Inc employee and a shareholder of Roche.

Acknowledgements

Notes and references

1 Y. Hu, J. Chen, G. Hu, J. Yu, X. Zhu, Y. Lin, S. Chen and J. Yuan, *Mar. Drugs*, 2015, **13**, 202–221.

2 C. Jiménez, *ACS Med. Chem. Lett.*, 2018, **9**, 959–961.

3 L. R. H. Krumpe, B. A. P. Wilson, C. Marchand, S. N. Sunassee, A. Bermingham, W. Wang, E. Price, T. Guszczynski, J. A. Kelley, K. R. Gustafson, Y. Pommier, K. J. Rosengren, C. I. Schroeder and B. R. O'Keefe, *J. Am. Chem. Soc.*, 2020, **142**, 21178–21188.

4 A. Zakharenko, N. Dyrkheeva and O. Lavrik, *Med. Res. Rev.*, 2019, **39**, 1427–1441.

5 T. M. Khomenko, A. L. Zakharenko, A. A. Chepanova, E. S. Ilina, O. D. Zakharova, V. I. Kaledin, V. P. Nikolin, N. A. Popova, D. V. Korchagina, J. Reynisson, R. Chand, D. M. Ayine-Tora, J. Patel, I. K. H. Leung, K. P. Volcho, N. F. Salakhutdinov and O. I. Lavrik, *Int. J. Mol. Sci.*, 2019, **21**, 126.

6 E. Schwarz, *Biol. Chem.*, 2017, **398**, 1295–1308.

7 N. L. Daly and D. J. Craik, *Curr. Opin. Chem. Biol.*, 2011, **15**, 362–368.

8 P. E. Dawson, T. W. Muir, I. Clark-Lewis and S. B. Kent, *Science*, 1994, **266**, 776–779.

9 G.-M. Fang, Y.-M. Li, F. Shen, Y.-C. Huang, J.-B. Li, Y. Lin, H.-K. Cui and L. Liu, *Angew. Chem., Int. Ed.*, 2011, **50**, 7645–7649.

10 J.-S. Zheng, S. Tang, Y.-K. Qi, Z.-P. Wang and L. Liu, *Nat. Protoc.*, 2013, **8**, 2483–2495.

11 P. Chakrabarti and J. Janin, *Proteins: Struct., Funct., Bioinf.*, 2002, **47**, 334–343.

12 D. Talavera, D. L. Robertson and S. C. Lovell, *PLoS One*, 2011, **6**, e21053.

13 L. Braunschweiler and R. R. Ernst, *J. Magn. Reson.*, 1983, **53**, 521–528.

14 J. Jeener, B. H. Meier, P. Bachmann and R. R. Ernst, *J. Chem. Phys.*, 1979, **71**, 4546–4553.

15 R. L. J. Keller, *The computer aided resonance assignment tutorial*, CANTINA Verlag, 1st edn, 2004.

16 K. Wüthrich, *NMR of proteins and nucleic acids*, John Wiley & Sons, New York, 1986.

17 C. I. Schroeder and K. J. Rosengren, *Methods Mol. Biol.*, 2020, **2068**, 129–162.

18 D. Wishart, C. Bigam, A. Holm, R. Hodges and B. Sykes, *J. Biomol. NMR*, 1995, **5**, 67–81.

19 Y. Shen and A. Bax, *J. Biomol. NMR*, 2013, **56**, 227–241.

20 T. Cierpicki and J. Otlewski, *J. Biomol. NMR*, 2001, **21**, 249–261.

21 P. Güntert, *Methods Mol. Biol.*, 2004, **278**, 353–378.

22 A. T. Brünger, *Nat. Protoc.*, 2007, **2**, 2728–2733.

23 V. B. Chen, W. B. Arendall, J. J. Headd, D. A. Keedy, R. M. Immormino, G. J. Kapral, L. W. Murray, J. S. Richardson and D. C. Richardson, *Acta Crystallogr., Sect. D: Biol. Crystallogr.*, 2010, **66**, 12–21.

24 R. Koradi, M. Billeter and K. Wüthrich, *J. Mol. Graphics*, 1996, **14**, 51–55.